

Thermal, Structural, and Mechanical Effects of Nanofibrillated Cellulose in Polylactic Acid Filaments for Additive Manufacturing

Diego Gomez-Maldonado,^a Maria Soledad Peresin,^a Christina Verdi,^b Guillermo Velarde,^b and Daniel Saloni^{b,*}

As the additive manufacturing process gains worldwide importance, the need for bio-based materials, especially for in-home polymeric use, also increases. This work aims to develop a composite of polylactic acid (PLA) and nanofibrillated cellulose (NFC) as a sustainable approach to reinforce the currently commercially available PLA. The studied materials were composites with 5 and 10% NFC that were blended and extruded. Mechanical, structural, and thermal characterization was made before its use for 3D printing. It was found that the inclusion of 10% NFC increased the modulus of elasticity in the filaments from 2.92 to 3.36 GPa. However, a small decrease in tensile strength was observed from 55.7 to 50.8 MPa, which was possibly due to the formation of NFC aggregates in the matrix. This work shows the potential of using PLA mixed with NFC for additive manufacturing.

Keywords: Biocomposites; Cellulose nanofibrils; Polylactic acid; Thermal properties; Mechanical properties; Additive manufacturing; 3D printing.

Contact information: a: Forest Products Development Center, School of Forestry and Wildlife Science, Auburn University, 520 Devall Dr., Auburn, AL 36849 USA; b: Department of Forest Biomaterials, North Carolina State University, Box 8005, Raleigh, NC 27695-8005 USA;

* Corresponding author: desaloni@ncsu.edu

INTRODUCTION

Additive manufacturing, which is also known as 3D printing, is a rapidly emerging manufacturing process in which components are fabricated directly from computer models by selectively depositing and consolidating raw materials in successive layers (Holmström *et al.* 2010; Calignano *et al.* 2017). Currently, the polymer-based additive manufacturing industry is based on the use of petroleum-based filaments that can be used in processes such as injection molding. These filaments are traditionally made of materials such as acrylonitrile butadiene styrene (ABS), polycarbonate, and Nylon (Goodship *et al.* 2015). However, biopolymers that are more sustainable, such as polylactic acid (PLA), have started to gain traction as a competitor to these traditional synthetic polymers.

The so-called sustainability of PLA comes from its production from corn starch and its biodegradability in composted conditions (Lunt 1998; Siracusa *et al.* 2008; Mülhaupt 2013). This is further favored by its lower hot end extrusion temperatures and reduced residual stress when compared with other competitive synthetic polymers, especially with its main competitor, ABS (Casavola *et al.* 2017). These milder conditions also result in printings with less warping and other layer defects in unheated chambers, along with an absence of released fumes (Wittbrodt and Pearce 2015).

Previous literature shows that printed ABS has relatively consistent tensile strength once printed, between 27.6 to 29.7 MPa, while PLA varies depending on the number of layers used and orientation in which it was printed varying from 30 to 63 MPa (Tymrak *et al.* 2014). Furthermore, this variation was also observed when composites with wood fiber biocomposite (Le Duigou *et al.* 2016), carbon fiber (Tian *et al.* 2016), or other fillers involving crosslinking (Davidson *et al.* 2016) were tested. However, the addition of these materials decreased the variation and improved the overall mechanical properties as PLA serves as a matrix.

As mentioned before, the main advantage of the use of PLA is its inherent suitability; nevertheless, this formation of composites to improve the mechanical properties should be then limited to the use of other bio-based polymers to maintain this advantage over the commercially available synthetic-base polymers. For this, cellulose, and especially cellulose nanomaterials, are the perfect candidates.

As a bio-based material, cellulose is the most abundant polysaccharide with a natural estimated biosynthesis of 1.5×10^{12} annual tons (Gilbert and Kadla 1998; Klemm *et al.* 2002). This polymer is generated by β -D-glucopyranose monomers linked through acetal bonds on the carbons in position C1 and C4, which forms a linear polymer with a high tendency to form hydrogen bonds between units and adjacent chains that form nanofibrils (10 to 30 nm) or microfibers (> 100 nm) (Klemm *et al.* 2005). In addition to their natural origin, these cellulose nanomaterials have high tensile strength with small variations depending on the origin, extraction process, and purity; with values ranging between 95 MPa when extracted from wood (Karim *et al.* 2016) and 200 to 300 MPa from the more pure bacterial nanocellulose (Yamanaka 1994).

Furthermore, cellulose and PLA composites have been previously studied with good results in bulk and films (Klemm *et al.* 2005a; Mathew *et al.* 2005; Graupner *et al.* 2009; Suryanegara *et al.* 2009; Jonoobi *et al.* 2010; Frone *et al.* 2013). However, to the best of the authors' knowledge the study in the formation of the filaments with these materials is limited (Blaker *et al.* 2014; Dong *et al.* 2017; Li *et al.* 2018; Murphy and Collins 2018), with most of them studying modified or polymerized cellulose (Dong *et al.* 2017; Li *et al.* 2018), from not wood-derived nanofibers (Blaker *et al.* 2014), or with microcrystalline cellulose instead of nanofibers (Murphy and Collins 2018). Therefore, this work aims to design, evaluate, and characterize filaments from PLA reinforced with wood-derived cellulose nanofibrils, hoping to increase the knowledge suitable for this innovative application of additive manufacturing that is being considered by many as the new industrial revolution.

EXPERIMENTAL

Materials

PLA (Ingeo™ Biopolymer 4043D) 3D printing monofilament grade was supplied by NatureWorks LLC (Minnetonka, MN, USA). The PLA was transparent, with a specific gravity of 1.24 g/cm³ and a melt flow index of 6 g/10 min. Freeze-dried cellulose nanofibril powder (NFC, 98% w/w) was obtained from the Process Development Center (PCD) from University of Maine (Orono, ME, USA). The NFC have a reported nominal fiber width of 50 nm, a surface area of 31 to 33 m²/g (Brunauer-Emmett-Teller (BET) surface area), and a density of 1.5 g/cm³.

PLA and NFC Composite Formation

Samples were processed based on the methods described by Saloni and Mervine (2020). Briefly, PLA was mixed with dried NFC in two concentrations (5 and 10% w/w) through hot-melt compounding in a Microcompounder MC15 (Xplore Instruments BV, Sittard, Netherlands). For the composite formation, 10 g of total mass was mixed at 150 °C and 120 rpm for 10 min. Afterwards, the mixture was pulverized and sifted through a Hogentogler No. 6 mesh sieve (Columbia, MD, USA) to ensure a consistent size.

Filament Extrusion

Before extrusion, preliminary tests were done to assess the best nozzle sizes to avoid excess swelling and obtain filaments with diameters acceptable for the printing equipment.

Then, prior to extrusion, the materials were oven-dried at 100 °C for 24 h to eliminate residual moisture. After, a preheated extruder from Filastruder (Snellville, GA, USA) was set with a nozzle of 1.75 mm diameter and 170 °C for PLA; while for the PLA-NFC composite blend a nozzle of 1.90 mm and 160 °C were used.

Printing Parameters

Printing configurations were based on those used by Saloni and Mervine (2020). All prints were made using a Fusion3 F306 3D Printer (Greensboro, NC, USA) along with Simplify3D software (Simplify3D, version 4.1.2, Cincinnati, OH, USA) as the slicing software. The printer was set to a print speed of 50 mm/s, two perimeter walls, and rectilinear infill pattern at alternating 45° angles based on the layer of the part. The extrusion width for all samples was 0.45 mm and the bed temperature was 45 °C. The only modified setting was the nozzle temperature, which was 215 and 205 °C for PLA and PLA-NFC, respectively.

Testing samples were printed based on the specific needs of the tests to be performed. Thus, the tensile, thermogravimetric analysis (TGA), and differential scanning calorimetry (DSC) samples were printed at 100% infill. Meanwhile, the print quality samples were printed at 25% infill to match more commonly used 3D printing settings.

Methods

TGA

The formed filaments and the composite blend were tested in a PE Pyris 1 TGA from PerkinElmer (Waltham, MA, USA). For these tests, between 5 and 10 mg were placed in platinum pans under air atmosphere and the temperature were evaluated from room 20 to 500 °C with temperature rate of 10 °C/min. The collected data was processed with Pyris software (PerkinElmer, version 11.1.0.0488, Waltham, MA, USA).

DSC

The DSC data from filaments and composites were recorded with a Diamond differential scanning calorimeter with Intercooler from PerkinElmer (Waltham, MA, USA). For these tests, samples of 3 and 5 mg were sealed in aluminum pans. The scanning rate was of 10 °C/min within the range of 25 to 220 °C with two cycles under a nitrogen atmosphere delivered at a 50 mL/min rate. All data calculations were developed in the Pyris software. To avoid thermal history, only the second cycle obtained is herein presented.

Tensile strength

The formed filaments were placed in an MTS Insight Electromechanical Testing System (Eden Prairie, MN, USA). All tests were performed with a crosshead speed of 25 mm/min and a grip dimension of 100 mm.

Scanning electron microscopy (SEM)

The formed filaments were placed on standard aluminum sample stubs using carbon tape and coated with 7 nm of Au/Pd (60/40) in a Technics Hummer II sputter coater from Anatech (Sparks, NV, USA). Images were collected at 2500X (10 μm marker shown) magnification using a Hitachi S-3200N SEM (Ibaraki, Japan) under high vacuum conditions with a 5 keV electron beam

RESULTS AND DISCUSSION

PLA-NFC Composite

After the formation of the blend, thermal characterization of the composite was performed before using it to form the filament to better understand the possible modifications after the extrusion process.

In the thermograms presented in Fig. 1, a decrease on the onset temperatures can be observed from 307.5 $^{\circ}\text{C}$ to 286.9 $^{\circ}\text{C}$ when the concentration of NFC increased compared to the pure PLA. Similarly, the maximum degradation temperature decreased as the concentration of NFC increased. These results are consistent with what was observed using grafted cellulose with PLA (Dong *et al.* 2017).

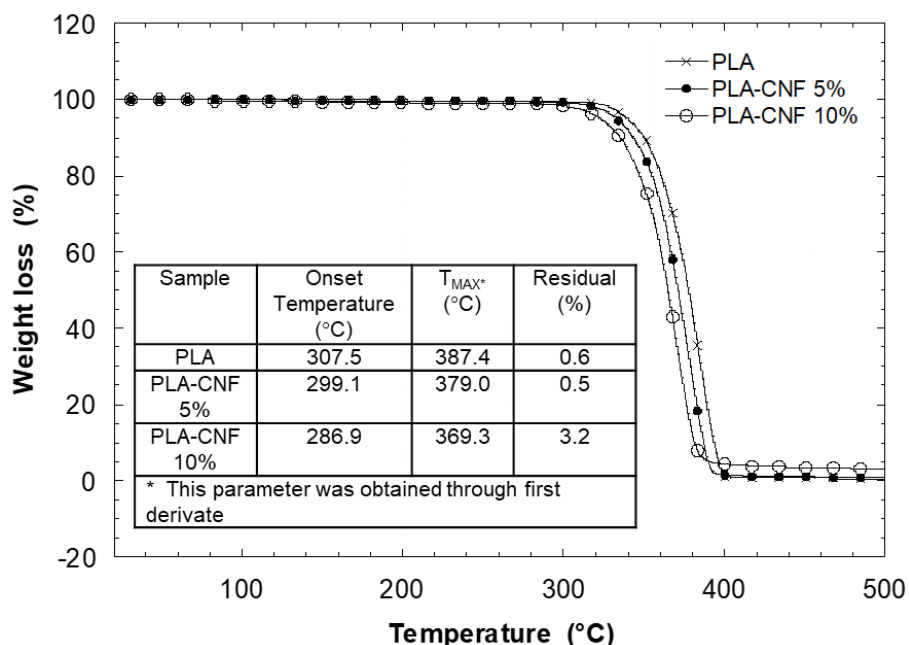


Fig. 1. Thermograms of PLA and its composite derivatives with NFC, PLA-NFC 5%, and PLA-NFC 10%; inset table shows the temperature parameters for the composite materials

Meanwhile, DSC data (Fig. 2) showed less variation in the behavior of the samples. The main observable difference was the change in the initial slope that became steadier as

the concentration of NFC increased in the samples. This finding was consistent with the observations done with the grafted cellulose (Dong *et al.* 2017).

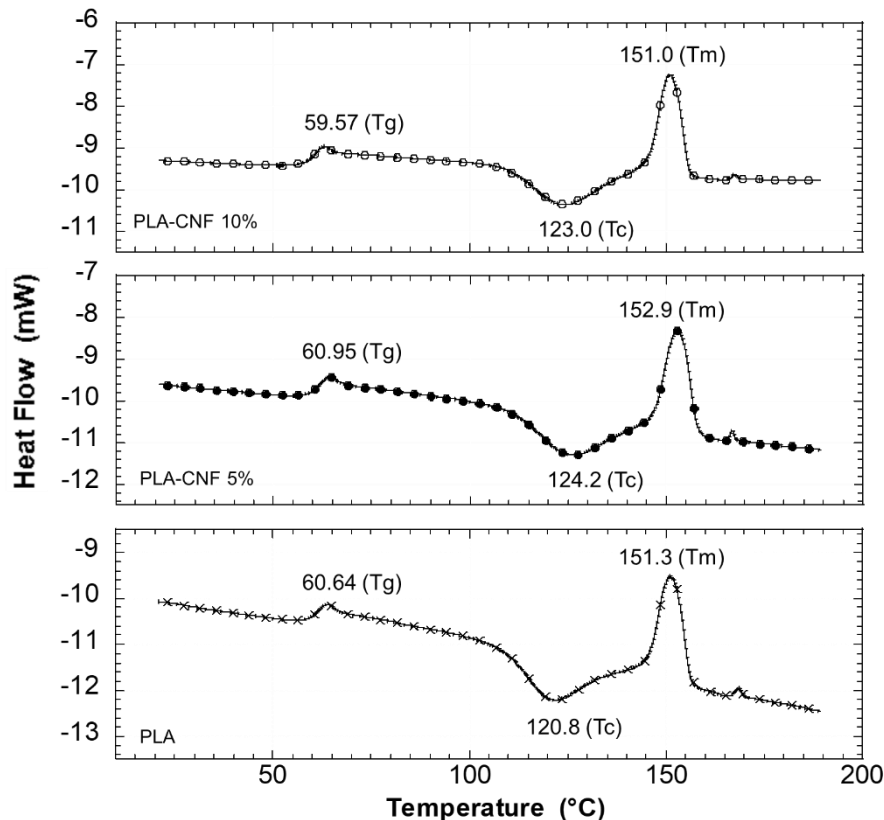


Fig. 2. DSC curves of the PLA and the composites generated with cellulose nanofibrils, PLA-NFC 5%, and PLA-NFC 10%. In the curves, peaks were assigned to the corresponding temperatures transitions: glass transition (T_g), crystallization (T_c), and melting (T_m).

PLA-NFC Filaments

After formation, the filament formed from pure PLA had an average diameter of 1.68 ± 0.07 mm. In contrast, PLA-NFC composites had smaller extruded diameter average of 1.62 ± 0.07 mm. This decrease in diameter can be attributed to aggregates on the NFC that decreased the surface area, forming more compact areas with the same mass (Jonoobi *et al.* 2010).

To further assess the formation of the filaments, images of the cross-section were obtained by SEM (Fig. 3). In them, it was observed that some aggregation was present in the filaments made from the composite blends with NFC, similar to other PLA-NFC composites reported in the literature (Jonoobi *et al.* 2010; Blaker *et al.* 2014). Furthermore, the smoothness of the surface changed with the increments on NFC, resulting in a clear phase separation in the filament made with 10% NFC, probably due to poor interfacial bonding between the NFC agglomerates and the matrix.

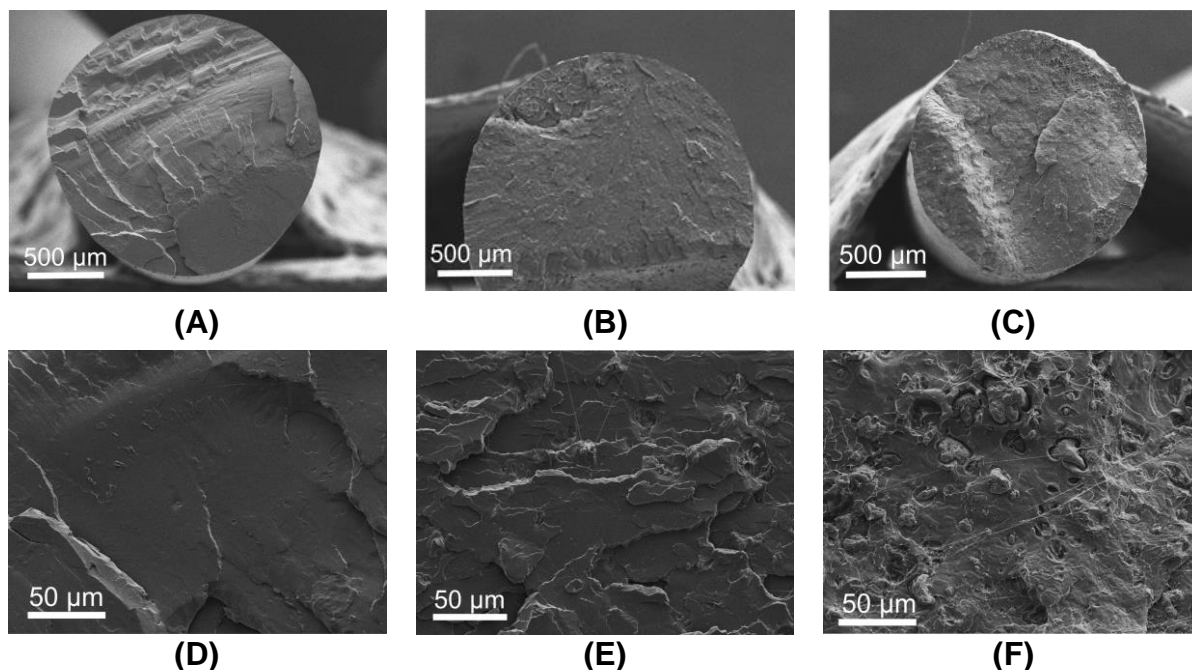


Fig. 3. Images of a cross-section of the filaments obtained through SEM, at 500 μm and 50 μm magnification. Herein, (A) and (D) are the PLA filament, (B) and (E) are PLA-NFC 5%, while (C) and (F) PLA-NFC 10%.

When the filaments were tested to characterize their mechanical properties (Table 1), it was found that the addition of the NFC to the material increased the modulus of elasticity for the filament from 2.92 to 3.36 GPa for the PLA to the PLA-NFC 10%, respectively. Showing that the presence of NFC helped to increase the resistance of the filament to deformation as the cellulose chains content increased in the matrix.

However, there was a decrease in the tensile strength and the maximum strain that the filament supported, which again could be related to aggregation of NFC in the matrix that was observed in Fig. 3. These decreases are coherent with the presence of the NFC, as the presence of NFC increases the stiffness of the composites, that with the formation of aggregates, the low orientation and poor interfacial bonding lead to an easier break of the filaments (Clarkson *et al.* 2019).

Table 1. Mechanical Properties of the PLA and PLA-NFC Filaments

Materials	Tensile Strength (MPa)	Modulus of Elasticity (GPa)	Max Strain (%)
PLA	55.7	2.92	2.80
PLA-NFC 5%	49.9	3.08	2.25
PLA-NFC 10%	50.9	3.36	2.20

As stated above, the thermal analysis of the filaments was performed (Fig. 4A). A slight decrease in the onset temperature on the PLA can be noted when it is in its free form and in the filament, from 307.5 to 300.2 $^{\circ}\text{C}$. However, this tendency was contrary for the composite materials that increased between 1 and 2 $^{\circ}\text{C}$. For PLA and PLA-NFC 5% the T_{MAX} decreased slightly, while for the PLA-NFC 10% it was maintained, this could be related to more aggregates of NFC that keep the material dispersed.

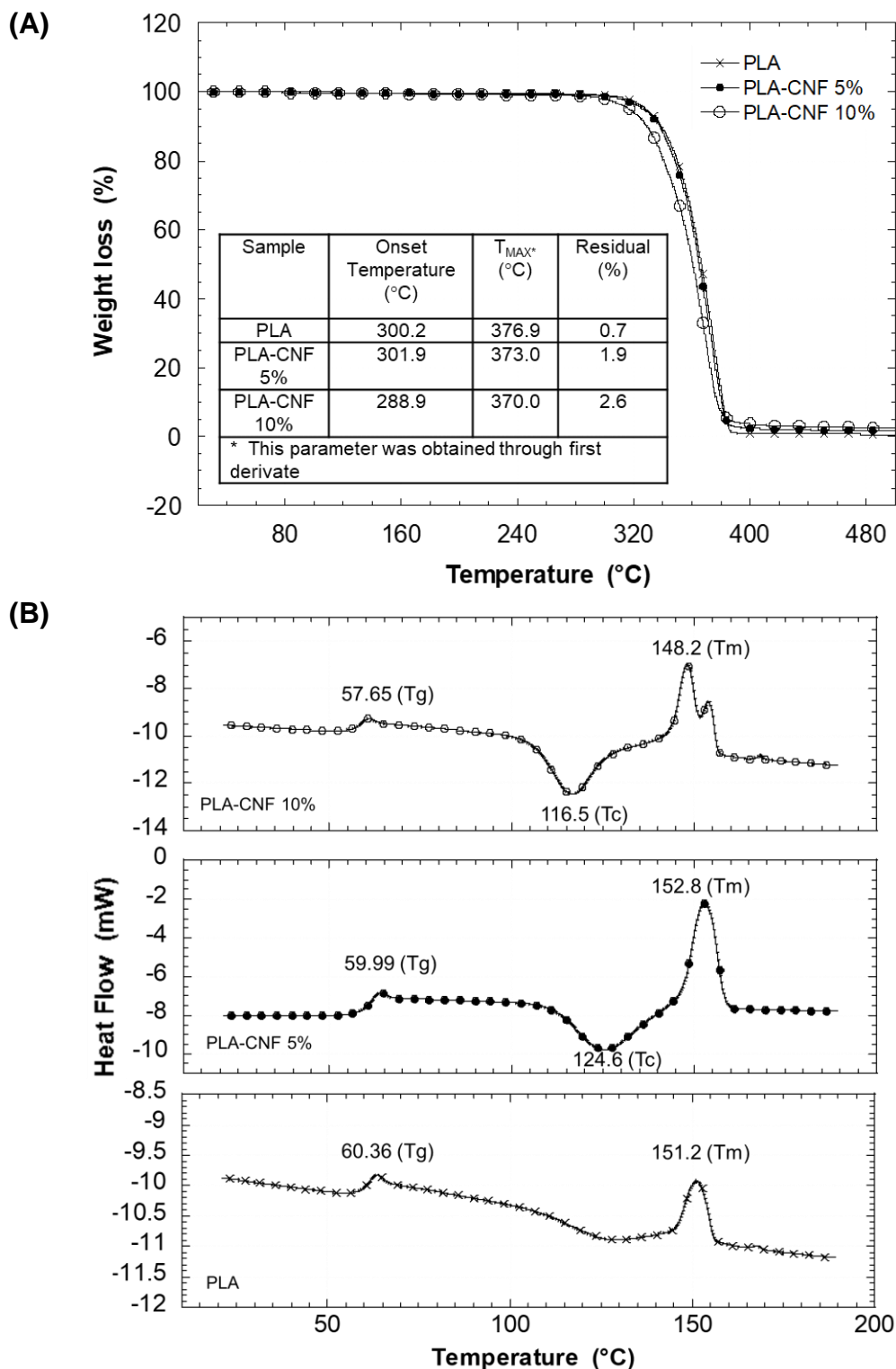


Fig. 4. (A) Thermograms of the filaments obtained from PLA and its composite with NFC: PLA-NFC 5% and PLA-NFC 10%. Inset table shows the temperature parameters for the composite materials. (B) DSC curves of the same filaments; peaks were assigned to the corresponding temperature transitions: glass transition (T_g), crystallization (T_c), and melting (T_m)

For the DSC data (Fig. 4B), PLA after extrusion did not present a clear crystallization peak compared to the curve obtained from the composite alone. However, a bigger difference was presented in the PLA-NFC 10% filament, where it presents two melting peaks, which further confirms the formation of clusters in the filament formation and dilucidated a poor interfacial bonding between the two materials.

3D Print Model

A print sample was performed with the PLA-NFC 5% as a proof of concept and compared with a printed version of the same model with the pure PLA filament. The samples are presented in Fig. 5, where it can be observed an accurate resolution after the printing, as well as consistency in the appearance.

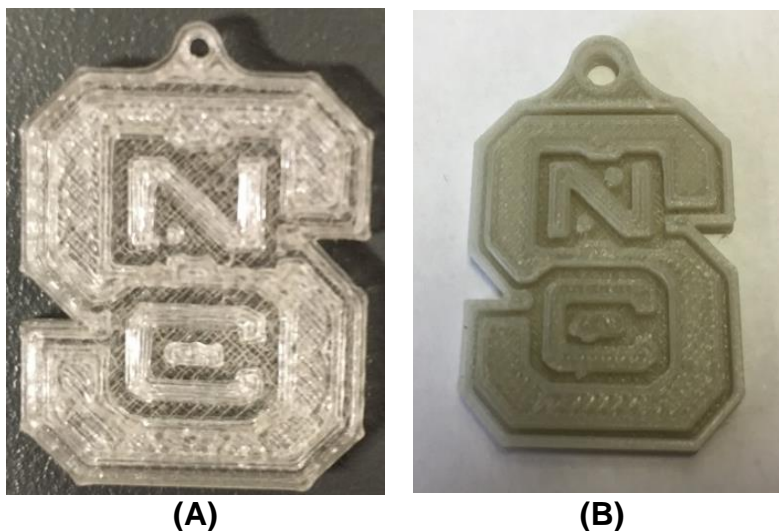


Fig. 5. 3D printed version of the NC State University logo with (A) PLA and (B) PLA-NFC 5%

As a first approximation, this printing proved that the use of these composite materials is feasible for 3D printing. Furthermore, it was observed that the increase in NFC content improved the modulus of elasticity of the samples. In this work, only the 5% concentration was utilized, and it was assumed that if more homogeneous filaments are obtained, better properties could be obtained.

CONCLUSIONS

1. In this work, composites and filaments of poly(lactic acid) (PLA) and nanofibrillated cellulose (NFC) were obtained without extra chemical modification.
2. Compounding and extrusion effectively occurred at 5% and 10% concentration of NFC. Extruded filament diameter for PLA and PLA-NFC had low standard deviation. In addition, PLA-NFC 5% filament was successfully used to print a 3D structure with similar conditions to the pure PLA filament.
3. The presence of NFC seemed to have a positive impact on the modulus of elasticity of the filaments. However, a slight decrease in tensile strength was observed possibly due to the presence of aggregates of NFC in the matrix.

4. 3D printed parts with PLA + NFC composites were comparable with pure PLA in terms of surface quality, an absence of visible delamination, visual flatness, and general appearance. Printing parameters and conditions were the same for both materials for consistency in the comparison.

ACKNOWLEDGMENTS

The authors are grateful for the support provided by the Wood-Based Composites Center, a National Science Foundation Industry/University Cooperative Research Center (Award 1624536-IIP). Additionally, this publication was supported by the Alabama Agricultural Experiment Station, and the Hatch program of the National Institute of Food and Agriculture, United States Department of Agriculture. The School of Forestry and Wildlife Sciences at Auburn University financial support to complete this work is greatly appreciated.

REFERENCES CITED

- Blaker, J. J., Lee, K. Y., Walters, M., Drouet, M., and Bismarck, A. (2014). "Aligned unidirectional PLA/bacterial cellulose nanocomposite fibre reinforced PDLLA composites," *Reactive and Functional Polymers* 85, 185-192. DOI: 10.1016/j.reactfunctpolym.2014.09.006
- Calignano, F., Manfredi, D., Ambrosio, E. P., Biamino, S., Lombardi, M., Atzeni, E., Salmi, A., Minetola, P., Iuliano, L., and Fino, P. (2017). "Overview on additive manufacturing technologies," *Proceedings of the IEEE* 105(4), 593-612. DOI: 10.1109/JPROC.2016.2625098
- Casavola, C., Cazzato, A., Moramarco, V., and Pappaletta, G. (2017). "Preliminary study on residual stress in FDM parts," in: *Residual Stress, Thermomechanics & Infrared Imaging, Hybrid Techniques and Inverse Problems*, Vol. 9, Springer International Publishing, New York, NY, USA, pp. 91-96. DOI: 10.1007/978-3-319-42255-8_12
- Clarkson, C. M., El Awad Azrak, S. M., Chowdhury, R., Shuvo, S. N., Snyder, J., Schueneman, G., Ortalan, V., and Youngblood, J. P. (2019). "Melt spinning of cellulose nanofibril/polylactic acid (NFC/PLA) composite fibers for high stiffness," *ACS Appl. Polym. Mater.* 1(2), 160-168, DOI:10.1021/acsapm.8b00030.
- Davidson, J. R., Appuhamillage, G. A., Thompson, C. M., Voit, W., and Smaldone, R. A. (2016). "Design paradigm utilizing reversible Diels-Alder reactions to enhance the mechanical properties of 3D printed materials," *ACS Applied Materials & Interfaces* 8(26), 16961-16966. DOI: 10.1021/acsami.6b05118
- Dong, J., Li, M., Zhou, L., Lee, S., Mei, C., Xu, X., and Wu, Q. (2017). "The influence of grafted cellulose nanofibers and postextrusion annealing treatment on selected properties of poly(lactic acid) filaments for 3D printing," *Journal of Polymer Science, Part B: Polymer Physics* 55(11), 847-855. DOI: 10.1002/polb.24333
- Le Duigou, A., Castro, M., Bevan, R., and Martin, N. (2016). "3D printing of wood fibre biocomposites: From mechanical to actuation functionality," *Materials & Design* 96, 106-114. DOI: 10.1016/j.matdes.2016.02.018
- Frone, A. N., Berlioz, S., Chailan, J. F., and Panaitescu, D. M. (2013). "Morphology and

- thermal properties of PLA-cellulose nanofibers composites,” *Carbohydrate Polymers* 91(1), 377-384. DOI: 10.1016/j.carbpol.2012.08.054
- Gilbert, R. D., and Kadla, J. F. (1998). “Polysaccharides — Cellulose,” in: *Biopolymers from Renewable Resources*, Springer Berlin Heidelberg, Berlin, Germany, pp. 47–95. DOI: 10.1007/978-3-662-03680-8_3
- Goodship, V., Middleton, B., and Cherrington, R. (2015). *Design and Manufacture of Plastic Components for Multifunctionality: Structural Composites, Injection Molding, and 3D Printing*, *Design and Manufacture of Plastic Components for Multifunctionality: Structural Composites, Injection Molding, and 3D Printing*, Elsevier Science, Amsterdam, Netherlands. DOI: 10.1016/C2014-0-00223-7
- Graupner, N., Herrmann, A. S., and Müssig, J. (2009). “Natural and man-made cellulose fibre-reinforced poly(lactic acid) (PLA) composites: An overview about mechanical characteristics and application areas,” *Composites Part A: Applied Science and Manufacturing* 40(6–7), 810-821. DOI: 10.1016/j.compositesa.2009.04.003
- Holmström, J., Partanen, J., Tuomi, J., and Walter, M. (2010). “Rapid manufacturing in the spare parts supply chain: Alternative approaches to capacity deployment,” *Journal of Manufacturing Technology Management* 21(6), 687-697. DOI: 10.1108/17410381011063996
- Jonoobi, M., Harun, J., Mathew, A. P., and Oksman, K. (2010). “Mechanical properties of cellulose nanofiber (NFC) reinforced polylactic acid (PLA) prepared by twin screw extrusion,” *Composites Science and Technology* 70(12), 1742-1747. DOI: 10.1016/j.compscitech.2010.07.005
- Karim, Z., Claudpierre, S., Grahn, M., Oksman, K., and Mathew, A. P. (2016). “Nanocellulose based functional membranes for water cleaning: Tailoring of mechanical properties, porosity and metal ion capture,” *Journal of Membrane Science* 514, 418-428. DOI: 10.1016/j.memsci.2016.05.018
- Klemm, D., Heublein, B., Fink, H. P., and Bohn, A. (2005a). “Cellulose: Fascinating biopolymer and sustainable raw material,” *Angewandte Chemie - International Edition* 44(22), 3358-3393. DOI: 10.1002/anie.200460587
- Klemm, D., Schmauder, H. P., and Heinze, T. (2002). “Cellulose,” in: *Biopolymers. Volume 6, Polysaccharides II, Polysaccharides from Eukaryotes*, E. J. Vandamme, S. de Baets, and A. Steinbüchel (eds.), Wiley-VCH, Weinheim, Germany, pp. 275-287.
- Li, X., Ni, Z., Bai, S., and Lou, B. (2018). “Preparation and mechanical properties of fiber reinforced PLA for 3D printing materials,” *IOP Conference Series: Materials Science and Engineering* 322(2), Article ID 022012. DOI: 10.1088/1757-899X/322/2/022012
- Lunt, J. (1998). “Large-scale production, properties and commercial applications of poly lactic acid polymers,” *Polymer Degradation and Stability* 59(1–3), 145-152. DOI: 10.1016/S0141-3910(97)00148-1
- Mathew, A. P., Oksman, K., and Sain, M. (2005). “Mechanical properties of biodegradable composites from poly lactic acid (PLA) and microcrystalline cellulose (MCC),” *Journal of Applied Polymer Science* 97(5), 2014-2025. DOI: 10.1002/app.21779
- Mülhaupt, R. (2013). “Green polymer chemistry and bio-based plastics: Dreams and reality,” *Macromolecular Chemistry and Physics* 214(2), 159-174. DOI: 10.1002/macp.201200439
- Murphy, C. A., and Collins, M. N. (2018). “Microcrystalline cellulose reinforced polylactic acid biocomposite filaments for 3D printing,” *Polymer Composites* 39(4),

- 1311–1320. DOI: 10.1002/pc.24069
- Saloni, D., and Mervine, N. (2020). “Investigation of bioplastics for additive manufacturing,” in: *Advances in Additive Manufacturing, Modeling Systems and 3D Prototyping*, Springer, Cham, Switzerland, pp. 365-376. DOI: 10.1007/978-3-030-20216-3_34
- Siracusa, V., Rocculi, P., Romani, S., and Rosa, M. D. (2008). “Biodegradable polymers for food packaging: A review,” *Trends in Food Science and Technology* 19(12), 634-643. DOI: 10.1016/j.tifs.2008.07.003
- Suryanegara, L., Nakagaito, A. N., and Yano, H. (2009). “The effect of crystallization of PLA on the thermal and mechanical properties of microfibrillated cellulose-reinforced PLA composites,” *Composites Science and Technology* 69(7–8), 1187-1192. DOI: 10.1016/j.compscitech.2009.02.022
- Tian, X., Liu, T., Yang, C., Wang, Q., and Li, D. (2016). “Interface and performance of 3D printed continuous carbon fiber reinforced PLA composites,” *Composites Part A: Applied Science and Manufacturing* 88, 198-205. DOI: 10.1016/j.compositesa.2016.05.032
- Tymrak, B. M., Kreiger, M., and Pearce, J. M. (2014). “Mechanical properties of components fabricated with open-source 3-D printers under realistic environmental conditions,” *Materials & Design* 58, 242-246. DOI: 10.1016/j.matdes.2014.02.038
- Wittbrodt, B., and Pearce, J. M. (2015). “The effects of PLA color on material properties of 3-D printed components,” *Additive Manufacturing* 8, 110-116. DOI: 10.1016/j.addma.2015.09.006
- Yamanaka, S. (1994). “Applications of bacterial cellulose,” in: *Cellulosic Polymers, Blends and Composites*, R. D. Gilbert (ed.), Hanser/Gardner, Munich, Germany, pp. 207-215.

Article submitted: June 17, 2020; Peer review completed: July 19, 2020; Revised version received and accepted: August 31, 2020; Published: September 3, 2020.
DOI: 10.15376/biores.15.4.7954-7964